*Aerosol and Air Quality Research,* 10: 185–192, 2010

ISSN: 1680-8584 print / 2071-1409 online
doi: 10.4209/aaqr.2009.11.0070

# Development and Performance Evaluation of Air Sampler with Inertial Filter for Nanoparticle Sampling

**Masami Furuuchi[1*], Kazunobu Eryu[1], Mizuki Nagura[1], Mitsuhiko Hata[1], Takaharu Kato[2], Naoko Tajima[2], Kazuhiko Sekiguchi[3], Kensei Ehara[4], Takafumi Seto[1], Yoshio Otani[1]**

[1] *Graduated School of Natural Science and Technology, Kanazawa University, Kakuma-machi, Kanazawa, Ishikawa 9201192, Japan*
[2] *Kanomax Japan Inc., Suita, Osaka 5650805, Japan*
[3] *Graduate School of Science and Engineering, Saitama University, Saitama, Japan*
[4] *NMIJ/AIST, 1-1-1 Umezono, Tsukuba, Ibaraki 305-8563, Japan*

## ABSTRACT

This paper describes the design and evaluation of an ambient air sampler consisting of a four-stage impactor and an inertial filter, for collecting various size fractions, including nano-particles, in a short sampling period. Impactor stages of $PM_{10}/PM_{2.5}/PM_1/PM_{0.5}$ were successfully devised with a reasonable accuracy in terms of cutoff size and slope of the collection efficiency curves. The designed inertial filter had an aerodynamic cutoff size of $d_{p50}$ ~65 nm with a satisfactory sharpness in classification. The total pressure drop of the sampler (hereinafter referred to as a "Nanosampler") was ~30 kPa at a flow rate of 40 L/min. The developed Nanosampler has advantages over currently available samplers such as LPI and nano-MOUDI, in terms of portability and loss of semi-volatile components in ultrafine particles by evaporation at a reduced pressure. Furthermore, the size distributions of the ambient particles measured with the Nanosampler compared favorably with those measured by the conventional instruments that are currently available on the market.

***Keywords:*** Nano-particles; Inertial filter; Impactor; Pressure drop.

## INTRODUCTION

To accurately evaluate the health effect of airborne particulates, it is necessary to determine the chemical composition of particles with respect to particle size. This is because the deposition site of inhaled particles changes with particle size, and the clearance time of the deposited particles varies depending on the deposition sites, leading to differences in toxicity, even for the same composition of particles. This information is particularly important for nanoparticles (smaller than 100 nm in diameter) but reliable data is very scarce. A large proportion of nanoparticles penetrate into the lung periphery, i.e., the alveolar region. Particles deposited in the alveoli are readily transferred to the blood and are then quickly dispersed throughout the body (Hinds, 1999; Bolch *et al.*, 2001).

Fine particles with diameters below 2–3 μm, or $PM_{2.5}$ in ambient air also frequently contain high levels of hazardous chemicals. This is particularly true for particles with a diameter of less than 1 μm (Spurny, 1999; Maynard and Pui, 2007). Consequently, the evaluation of the chemical characteristics of ultrafine and nanoparticles is especially important in understanding the impact of airborne particulates that enter the respiratory system on the general health of an individual.

In order to conduct various quantitative chemical analyses of atmospheric particles, a relatively large mass of particles, possibly in the order of mg, must be collected by collecting them from atmospheric air by filtration. Although particles smaller than 0.1 μm, i.e., nanoparticles, account for a large proportion of the total population, their mass is very small. Therefore, collecting a sufficient mass of atmospheric nanoparticles requires a long sampling time. A number of samplers are available for achieving this, low pressure impactors (LPI) (Hering *et al.*, 1978, 1979; Kauppinen and Hillamo *et al.*, 1989) and a nano-multi orifice uniform deposit impactor (nano-MOUDI) (Fang *et al.*, 1991; MSP, 2009). A differential mobility analyzer (DMA) (Knutdon and Whitby, 1975) may be used as a classifier followed by the collection of classified particles with a filter. However, all of these devices have drawbacks, which include a small sampling rate, a low charging efficiency for nanoparticles, the production of artifacts and the loss of unstable chemicals by evaporation due to the large pressure drop (Hata *et al.*, 2009).

* Corresponding author. Tel./Fax: +81-76-2344646
*E-mail address:* mfuru@t.kanazawa-u.ac.jp

The inertial filter was developed by Otani *et al.* (2007) as a technique to overcome these difficulties. The filter has significant advantages over other techniques, such as a nanometer-size cutoff ($d_{p50}$) diameter at a moderate pressure drop (< 20–30 kPa), as well as a sufficiently high sampling flow rate that permits the rapid collection of particles. The inertial filter consists of stiff fibers with diameters in the micrometer range, which are loosely packed in a nozzle which allows a rather large filtration velocity of ca. 10–50 m/s (Otani *et al.*, 2007). By selecting the appropriate filter structure and filtration conditions, i.e., filtration velocity, fiber diameter and fiber volume fraction, particles can be classified using inertial filters with a cutoff size between ca. 50–200 nm.

In this study, solid-plate impactor stages of $PM_{10}/PM_{2.5}/PM_1/PM_{0.5}$ were installed upstream of the inertial filter to permit different size fractions of atmospheric particles, including nanoparticles, to be collected. The design concept and the separation performance of the developed Nanosampler are described in the present paper. Furthermore, the Nanosampler was applied to collect ambient particles for evaluating the separation performance of atmospheric particles. The concentration and size distribution of the collected ambient particles were compared with those from currently available samplers such as high and low volume air samplers with $PM_1$, $PM_{2.5}$ and $PM_{10}$ inlets as well as the LPI.

## INERTIAL FILTER

Large particles are collected by a filter with inertial impaction at a high filtration velocity, while small particles are removed by Brownian diffusion. The measures for inertial impaction and Brownian diffusion are the Stokes number, *Stk*, and the Peclet number, *Pe*:

$$Stk = \frac{C_c \rho_p d_p^{\,2} u}{9 \mu d_f} \tag{1}$$

$$Pe = \frac{u d_f}{D} \tag{2}$$

where $C_c$ is the Cunningham slip correction factor, $\rho$ the particle density, $d_p$ the particle diameter, $u$ the filtration velocity, $\mu$ the viscosity, $d_f$ the fiber diameter, and $D$ the Brownian diffusivity of particles. The collection efficiency of a filter increases with increasing *Stk* and decreasing *Pe*. Therefore, a high filtration velocity and thin fibers are preferable for achieving a large inertial effect. The collection efficiency for larger particles increases with the filtration velocity while that for smaller particles decreases. By further increasing the filtration velocity, the collection efficiency curve approaches that of ideal classification with a $d_{p50}$ value in the nanometer to ultrafine size range. In this study, the inertial filters were designed using filtration theory based on a single fiber collection efficiency (Otani *et al.*, 2007; Eryu *et al.*, 2009) to achieve a nanometer cutoff size with a relatively low pressure drop (< 20–30 kPa), which is much lower than the pressure drop of currently available samplers for nanometer size particles, such as LPI (70–80 kPa) and nano-MOUDI (~60 kPa) (Fang *et al.*, 1991; Otani *et al.*, 2007).

## STRUCTURE OF THE NANOSAMPLER

Fig. 1 shows a schematic drawing and picture of the Nanosampler. The sampler consists of a four-stage impactor of $PM_{10}/PM_{2.5}/PM_1/PM_{0.5}$ and an inertial filter with an aerodynamic cutoff diameter of $d_{p50}$ ~65 nm. The sampler was designed to operate at a flow rate of 40 L/min, which allows both the sufficiently fast sampling of atmospheric nanoparticles and portability as a field sampling device. The designed sampling flow rate is more than twice that of commercial low-volume samplers (16.7 L/min) but less than that of high volume air samplers (500–1000 L/min). The advantage of the Nanosampler is that the sampling flow rate can be readily changed, depending on the needs in the field.

The specifications of each impactor stage are shown in Table 1. The filter diameter is 55 mm for all stages. Similar to other samplers, various types of filters, such as glass and quartz fiber filters, Teflon filters can be used depending on the end purposes. The air flow was designed to leave an impaction plate from the peripheral of the impaction plate and is similar to the Andersen cascade impactor.

The inertial filter is designed so that the webbed stainless steel fibers (Nippon Seisen Co. Ltd., felt type, SUS-304) are packed on a support of crossed 200-μm stainless steel wires in a plastic holder (polyoxymethylene, POM) (see Fig. 2), and the holder is placed in the throat of nozzle. Since the web of SUS fibers has a high mechanical strength, making it resistant to compression, the filter structure can be maintained at a high filtration velocity. The geometric mean diameter of the SUS fibers measured from SEM photographs is 9.8 μm ($\sigma_g$ = 1.1). The adoption of a filter holder facilitates the handling of samples and it can be easily replaced with a new holder on site without directly touching the fibers. The filter holder can be reused after cleaning and are also disposable. The specifications of the inertial filters are summarized in Table 2.

## MEASUREMENT OF PERFORMANCE OF THE NANOSAMPLER

### *Impactor Stages*

Fig. 3(a) shows the rig used to test the performance of the impactor stages. Four different sized PSL particles (1.005, 2.005, 5.125 and 10.04 μm, JSR, STADEX SC-103-S, SC-200-S / DYNOSPHERES SS-052-P, SS-103-P) (JSR, 2009) generated by means of a Collison-type atomizer and a nebulizer were used as the test aerosol. PSL particles were neutralized with a $^{241}$Am neutralizer and mixed with clean air by means of a membrane filter and then introduced to the individual stage of the impactor. The number concentrations of PSL particles at the inlet and outlet of the impactor were measured using a laser particle counter (*Kanomax Japan Inc*, TF-500). The collection efficiency $E(d_p)$ of the particles can be calculated using Eq. (3).

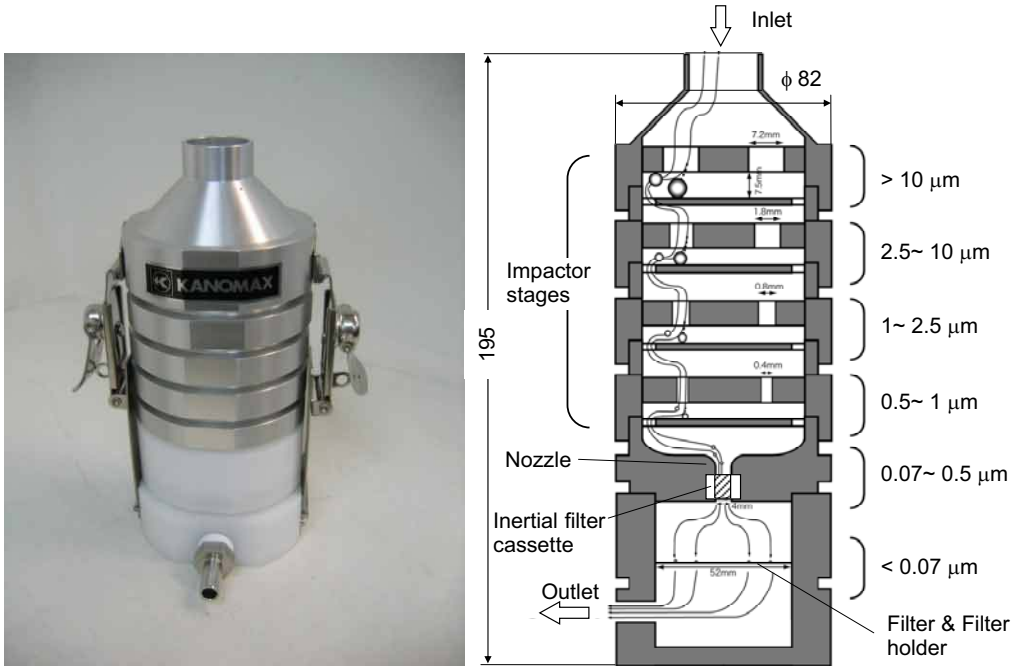


**Fig. 1**. Schematic drawing and picture of Nanosampler.

**Table 1.** Specifications of impactor stages.

| Stage | $PM_{10}$ | $PM_{2.5}$ | $PM_1$ | $PM_{0.5}$ |
|---|---|---|---|---|
| Nozzle diameter (mm) | 7.2 | 1.8 | 0.8 | 0.4 |
| Nozzle length (mm) | 7.5 | 3 | 2 | 2 |
| Nozzle-plate separation (mm) | 7.5 | 4.5 | 2 | 2 |
| Number of nozzles at each stage (-) | 6 | 25 | 50 | 100 |
| Diameter of impaction plate (mm) | 60 | 60 | 60 | 60 |
| Air velocity through nozzle (m/s) | 2.73 | 10.8 | 26.5 | 53.1 |
| $d_{p50}$ (μm) | | | | |
| Designed | 10 | 2.5 | 1 | 0.5 |
| Measured | 9.7 | 2.71 | 1.08 | 0.46 |
| Error (%) | –3 | 8 | 8 | –8 |

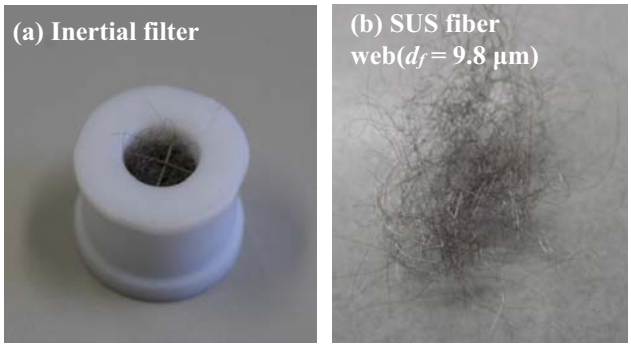


**Fig. 2.** Inertial filter cartridge along with SUS fiber web.tial filter cartridge along with SUS fiber web.

### *Inertial Filter*

Fig. 3(b) shows the experimental setup used to test the performance of the inertial filters. Zinc chloride ($ZnCl_2$) particles, generated using an evaporation-condensation type aerosol generator were used as the test aerosol. Zinc chloride was heated by an infrared ray image furnace (ULVAC, RHL-E25P) at a temperature between 260–320°C, and then cooled to produce particles. The generator is similar to those used in previous studies (Kousaka *et al.*, 1982; Okuyama *et al.*, 1986; Alonso *et al.*, 2004; Otani *et al.*, 2007). The monodisperse $ZnCl_2$ particles classified by DMA (TSI Inc., MODEL 3071) were diluted with clean air and then introduced to the inertial filter at a flow rate of 40 L/min. The collection efficiency based on particle number can be determined using an aerosol electrometer (TSI, Model 3068). The collection efficiency of particles was calculated using Eq. (3). The pressure drop through the inertial filter was measured by a digital manometer (Sokken, Model PE-33-A1).

A knowledge of the actual density of particles is necessary in order to convert the mobility equivalent diameter measured by the DMA, $d_p$, to the aerodynamic diameter, $d_{pa}$, i.e., $d_{pa} = \sqrt{\rho_p / \rho_{p0}} \cdot d_p$, where $\rho_{p0}$ = 1000 kg/m$^3$. Since the generated $ZnCl_2$ particles are aggregates of primary

**Table 2.** Specification of inertial filter.

| $d_f$ (μm) | Fiber material | Type | $L_n$ (mm) | $D_n$ (mm) | $Q$ (L/min) | Fiber loadings (mg) | Fiber volume fraction α (-) | Cutoff size (field test ) (mm) |
|---|---|---|---|---|---|---|---|---|
| 9.8 ($\sigma_g$ = 1.1) | SUS-304 | Webbed | 5.5 | 4.75 | 40 | 13–14 | 0.0135 | ~65 |

particles, their actual density may differ from that of the bulk material (the bulk density of $ZnCl_2$ is 2907 kg/m$^3$, (Perry, 1950)). Consequently, the actual density of the zinc chloride particles classified by the DMA was determined using an Aerosol Particle Mass Analyzer (*Kanomax Japan Inc*, APM 3600). The APM is capable of measuring the mass of an individual each particle down to 25 nm (Park *et al.*, 2004a, 2004b; Fukushima *et al.*, 2007; Lee *et al.*, 2009) as a result of the balance between centrifugal force and electrostatic force exerted on a charged particle. Fig. 3(c) shows the experimental setup used for the DMA-APM density measurement system. Polydisperse $ZnCl_2$ particles were classified with the DMA (TSI Inc., MODEL 3071), and then introduced to the APM. The number concentrations of particles escaping from the APM at various applied voltages were determined by means of a condensation particle counter (CPC, TSI Inc., MODEL 3022A) to obtain the particle mass distribution of the DMA-classified particles.

***Sampling of Ambient Particles***

In order to evaluate the separation performance of the

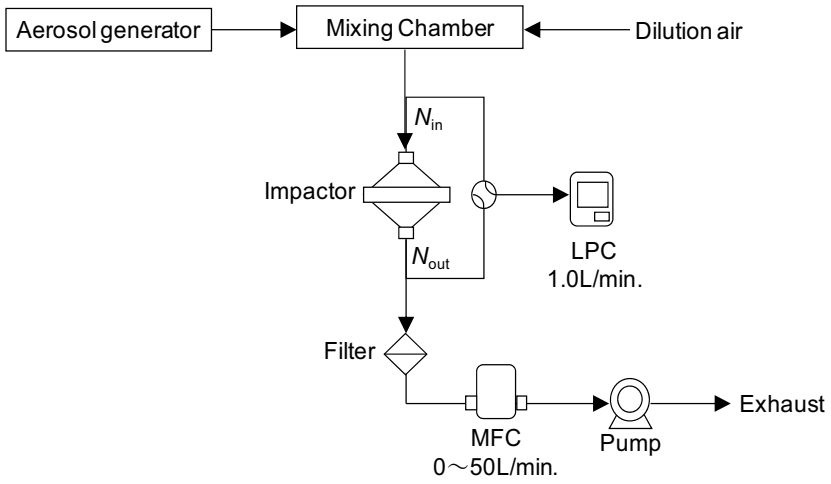


(a) Performance test of impactor stage.

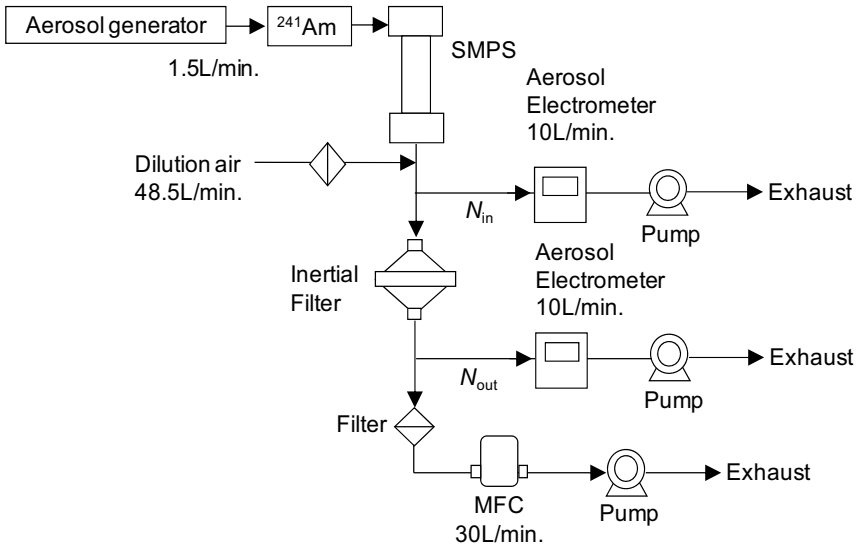


(b) Performance test of inertial filter

**Fig. 3.** Experiments setups: (a) the performance test of impactor stage, (b) the performance test of inertial filter, (c) the density measurement of $ZnCl_2$ particles.

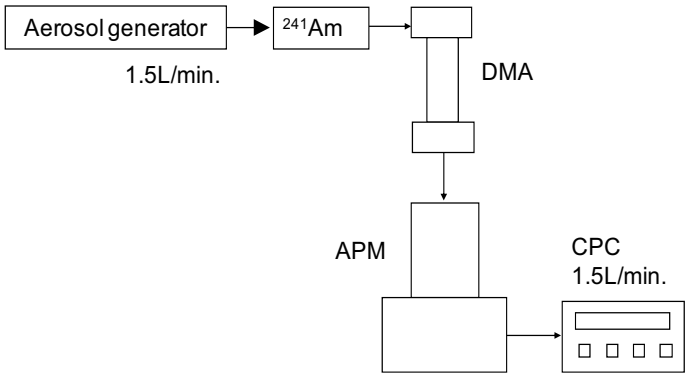


(c) Density measurement of $ZnCl_2$ particles.

**Fig. 3.** *(continued).*

Nanosampler for ambient particles, ambient aerosol particles were sampled with the Nanosampler simultaneously with currently available air samplers: a low pressure impactor (LPI, Tokyo Dylec, LP-20), a high volume air sampler (HV, Shibata, HV-1000F), a low volume air sampler (LV, R&P, Model 2000) with $PM_1$ and $PM_{2.5}$ EPA cyclone inlets and a TEOM particle mass monitor (R&P, TEOM1400) with a $PM_{10}$ EPA inlet. The sampling conditions are summarized in Table 3. Ambient particles were collected on quartz fiber filters (Pallflex, 2500QAT-UP) conditioned in a desiccator (room temperature, ~50% RH) for 48 hours before and after the sampling.

## RESULTS

### *Separation Performance of the Impactor Stages*

Fig. 4 shows collection efficiency curves for each impactor stage as a function of the aerodynamic diameter of particles. The corresponding experimental cutoff sizes ($d_{p50}$) are shown in Table 3, along with the designed values. The cutoff sizes of each stage are in good agreement with the designed ones with a reasonable slope in the collection efficiency curves. The total pressure drop through the four stage impactor was determined to be 5.4 kPa. This pressure drop is almost the same as that of the Andersen cascade impactor downstream from the final impactor stage with a cutoff size of $d_p$ = 0.43 μm.

### *Separation Performance of Inertial Filter*

Fig. 5 shows the density of $ZnCl_2$ particles measured with the APS as a function of the mobility equivalent diameter of particles classified by the DMA. The density is rather constant over the measured size range at a density between 1800–1900 kg/m$^3$, which is much smaller than the bulk density of zinc chloride (2907 kg/m$^3$, Perry, 1950). The mean density of 50–100 nm of singly charged $ZnCl_2$ particles generated at 320–350°C is 1870 kg/m$^3$. Consequently, this value was used to convert the mobility equivalent diameter to the aerodynamic diameter in the present study.

The collection efficiency curve of the inertial filter is shown in Fig. 4 as a function of aerodynamic diameter. The designed cutoff size of the inertial filer is $d_{p50}$ ~65 nm. The steepness of the classification curve is acceptable, although there is a slight increase in the collection efficiency for particles smaller than 30 nm because of Brownian diffusion. When the number concentration of particles in this size range is of interest, this increase in collection efficiency for small particles can be fatal. However, when the mass of particles smaller than 100 nm is of concern, as in the case of the chemical analysis of components in nano-particles, the particle mass below 20–30 nm occupies only a negligible portion of particle mass under 65 nm. The increase in collection efficiency may be avoided by increasing the filtration velocity with the sacrifice of a significant pressure drop. The measured pressure drop

**Table 3.** Sampling conditions.

| Equipments | Size range (μm) | Sampling period, term, number of samples | Flow rate (L/min) |
|---|---|---|---|
| Low pressure impactor (LPI) | 13 stages (>12 μm – <0.06 μm) | 28 days, Mar.–Jun., 2009, n = 3 | 24 |
| Low volume air sampler (LV) | $PM_{10}$, $PM_{2.5}$ (EPA cyclone inlets) | 4 days, Mar.–Jun., 2009, n = 5 | 16.7 |
| High volume air sampler (HV) | Total suspended particulates | 4 days, Mar.–Jun., 2009, n = 11 | 1000 |
| Tapered element oscillating microbalance | $PM_{10}$ | Every 10 minutes, Mar.–Jun., 2009 | Total: 16.7, Sensor flow rate: 2.0 |
| Nanosampler | 6 stages TSP/$PM_{10}$/$PM_{2.5}$/$PM_1$/$PM_{0.5}$/<65 nm | 4 days, Mar.–Jun., 2009, n = 11 | 40 |

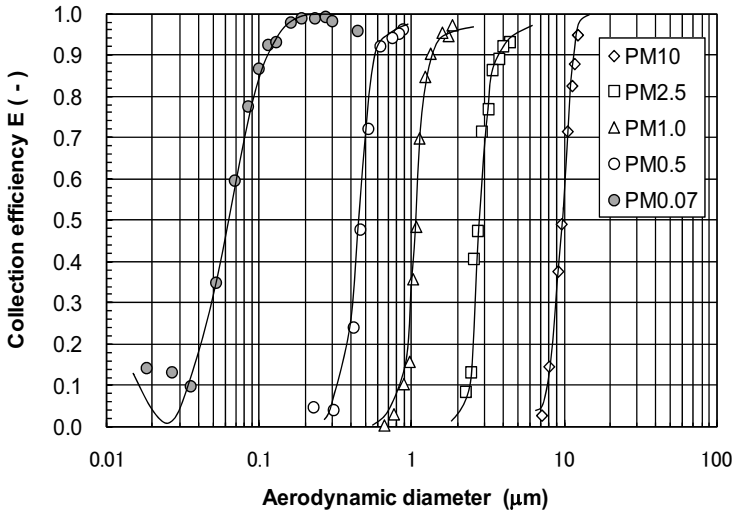


**Fig. 4.** Collection efficiency curves of the impactor stages and inertial filter.

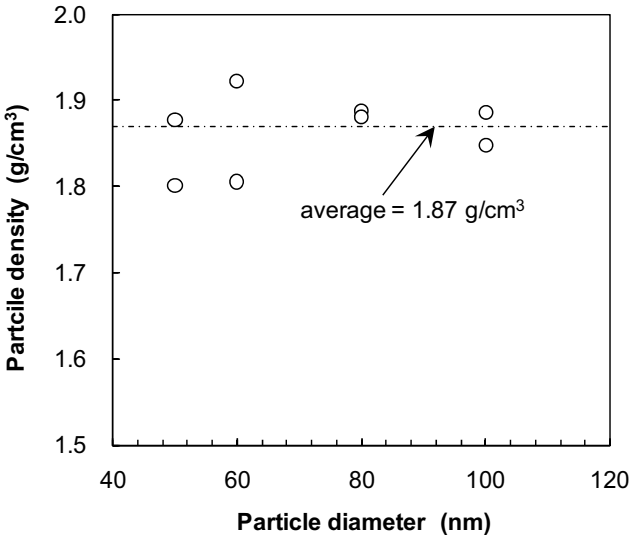


**Fig. 5.** Density of $ZnCl_2$ particles in relation to mobility equivalent diameter.

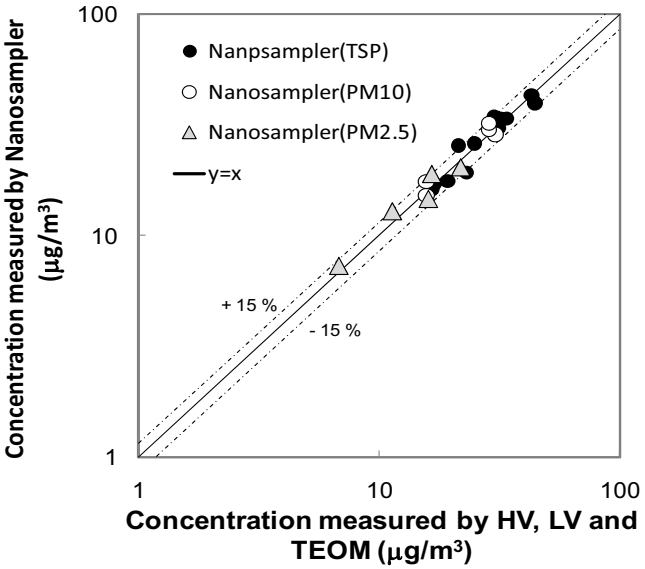


**Fig. 6.** Comparison of particle concentrations in different size ranges obtained by Nanosampler with those by other samplers.

though the inertial filter was ~25 kPa at a flow rate of 40 L/min. The pressure drop of a sampler with four-impactor stages and an inertial filter was ~30 kPa, which is much less than LPI (70–80 kPa) and nano-MOUDI (~60 kPa) with a 60–70 nm cutoff size. The total pressure drop of the sampler, including the sampler inlet and the backup filter, was ~33 kPa. Based on these results, it is possible to construct an air sampler consisting of a four-stage impactor and an inertial filter with a cutoff size of $d_{p50}$ = 100 nm at a total pressure of 10–15 kPa.

### *Ambient Particles*

Fig. 6 shows the relation between the concentrations of total suspended particles (TSP), $PM_{2.5}$ and $PM_{10}$ determined by the conventional instruments and the Nanosampler. The discrepancies between these samplers are less than ±15%, indicating that the separation performance of the impactor stages constructed in the present work are reliable. Cumulative size distributions on a mass basis obtained by the LPI and the Nanosampler are compared in Fig. 7. In general, a good agreement exists in the cumulative fraction between the different samplers, but there is a slight difference in the mass fraction of nanoparticles with sizes less than 0.1 μm. This can be attributed to the loss of semi-volatile components, such as nitrates, by evaporation, due to the large pressure drop in the case of LPI. This will be examined in detail in a future study, along with other chemical components such as poly-cyclic aromatic hydrocarbons.

## CONCLUSION

This paper describes the design and performance of an ambient air sampler consisting of a four-stage impactor and an inertial filter, for collecting various sized fractions including nano-particles in a sampling time shorter than currently available equipments such as LPI and nano-MOUDI.

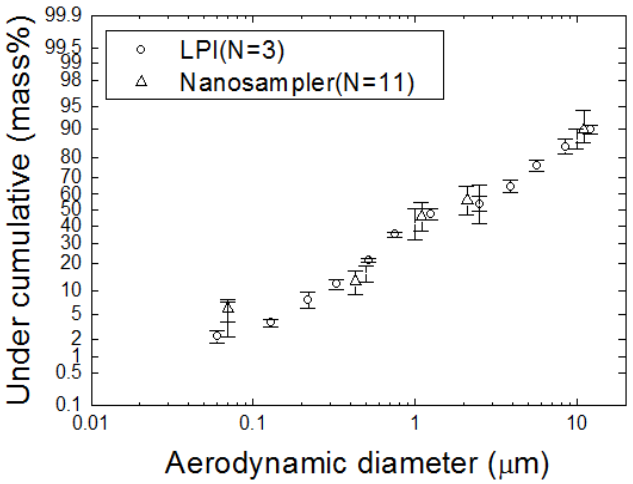


**Fig. 7.** Cumulative size distributions obtained by Nanosampler and the low pressure impactor (LPI).

Impactor stages of $PM_{10}/PM_{2.5}/PM_1/PM_{0.5}$ were successfully devised with a reasonable accuracy in cutoff size and the slope of in the collection efficiency curves. The designed inertial filter was shown to have an aerodynamic cutoff size of $d_{p50}$ ~65 nm with a satisfactory sharpness in classification. The total pressure drop of the Nanosampler was ~30 kPa at a flow rate of 40 L/min. This pressure drop allows the use of conventional pumps that are currently available on the market. As a result, the Nanosampler has advantages over currently available samplers such as the LPI and nano-MOUDI, in portability and loss of semi-volatile components in ultrafine particles by evaporation at reduced pressure.

The size distributions of ambient particles measured with the Nanosampler were compared favorably with those measured using conventional instruments that are currently available on the market. Detailed data measured with the present sampler will be reported in the near future. One of the important remaining issues of regarding the Nanosampler is the influence of particle load on the classification performance of the inertial filter, which may increase the pressure drop and change separation performance. These issues are currently being investigated and will be reported in the near future.

## ACKNOWLEDGEMENT

The authors gratefully acknowledge The Ministry of Economy, Trade and Industry (METI) for its support for this research (Research and development project for supporting small and medium enterprises). The authors also acknowledge Dr. Tsuji, National Metrology Institute of Japan (NMIJ), Advanced Institute of Science and Technology (AIST) for his great contribution on the performance measurement of the inertial filter.

## REFERENCES

Alonso, M. and Alguacil, F.J. (2004). Thin Coating on Ultrafine Aerosol Particles. Atmospheric Research. 82: 16th International Conference on Nucleation and Atmospheric Aerosols, December 2006, p. 605–609.

Bolch, W.E., Farfán, E.B, Huh, C., Huston, T.E., Bolch, W.E. (2001). Influence of Parameter Uncertainties within the ICRP 66 Respiratory Tract Model: Particle Deposition. *Health Phys.* 81:378–394.

Eryu, K., Seto, T., Mizukami, Y., Nagura, M., Furuuchi, M., Tajima, Y., Kato, T., Ehara, K. and Otani, Y. (2009). Design of Inertial Filter for Classification of $PM_{0.1}$. *J. Aerosol Res.* 24: 24–29. (in Japanese).

Fang, C.I., McMurry, P.H., Marple, V.A., and Rubow, K.L. (1991). Effect of Flow-induced Relative Humidity Changes on Size Cuts for Sulfuric Acid Droplets in the MOUDI. *Aerosol Sci. Tech.* 14: 266–277.

Fukushima, N., Ehara, K., Sakurai, H. and Coakley, K.J. (2007). Development of the Aerosol Particle Mass Analyzer, Proc. 25th Annual Tech. Meeting on Air Cleaning and Contamination Control, Tokyo. p. 128–130. (in Japanese).

Hata, M., Bai, Y., Furuuchi, M., Fukumoto, M., Otani, Y., Sekiguchi, K. and Tajima, N. (2009). Status and Characteristics of Ambient Aerosol Nano-particles in Kakuma, Kanazawa and Comparison between Sampling Characteristics of Air Samplers for Aerosol Particle Separation. *Bull. Jpn. Sea Res. Inst.* 40: 135–140. (in Japanese)

Hering, S.V., Flagan, R.C. and Fliedlander, S.K. (1978). Design and Evaluation of New Low-Pressure Impactor. *Environ. Sci. Technol.* 12: 667–673.

Hering, S.V., Fliedlander, S.K., Collins, J.J. and Richards, L.W. (1978). Design and Evaluation of a New Low-Pressure Impactor 2. *Environ. Sci. Technol.* 13: 184–188.

Hinds, W.C. (1999). *Aerosol Technology*, 2nd ed., Wiley-Interscience, New York.

JSR. (2009). http://www.jsr.co.jp/pd/fc_d05.shtml

Kauppinen, E.I. and Hillamo, R.E. (1989). Modification of the University of Washington Mark 5 in-stack Impactor. *J. Aerosol Sci.* 20: 813–827.

Kousaka, Y., Niida, T., Okuyama, K. and Tanaka, H. (1982). Development of a Mixing Type Condensation Nucleus Counter. *J. Aerosol Sci.* 13: 231–240.

Knutdon, E.O. and Whitby, K.T. (1975). Aerosol Classification by Electric Mobility: Apparatus, Theory, and Application. *J. Aerosol Sci.* 6: 443–451.

Lee, S.Y., Widiyastuti, W., Tajima, N., Iskandar, F. and Okuyama, K. (2009). Measurement of the Effective Density of Both Spherical Aggregated and Ordered Porous Aerosol Particles Using Mobility- and Mass-Analyzers. *Aerosol Sci. Tech.* 43: 36–144.

Marple, V.A. and Willeke, K. (1976). Inertial Impactors: Theory, Design and Use in Fine Particles. Edited by Liu, B.Y. H. *Academic Press, Inc*, p. 411–446.

Mayland, A.D. and Pui, D.Y.H. (2007). *Nanoparticles and Occupational Health*, Splinger, Dordrecht.

MSP. (2009). http://www.mspcorp.com/aero_products.php.

Okuyama, K., Kousaka, Y. and Hayashi, K. (1986). Brownian Coagulation of Two-component Ultrafine Aerosols. *J. Colloid Interface Sci.* 113: 42–54

Otani, Y., Eryu, K., Furuuchi, M., Tajima, N. and Tekasakul, P. (2007). Inertial Classification of Nanoparticles with Fibrous Filters. *Aerosol Air Qual. Res.* 7: 343–352.

Park, K., Kittelson, D.B. and McMurry, P.H. (2004a). Structural Properties of Diesel Exhaust Particles Measured by Transmission Electron Microscopy (TEM): Relationships to Particle Mass and Mobility. *Aerosol Sci. Technol.* 38: 881–889.

Park, K., Kittelson, D.B., Zachariah, M.R. and McMurry, P.H. (2004b). Measurement of Inherent Material Density of Nanoparticle Agglomerates. *J. Nanopart. Res.* 6: 267–272.

Perry, J.H. (1950). *Chemical Engineer's Handbook*, 3rd ed. McGraw-Hill, New York. p. 148.

Spurny, K.R. (1999). *Analytical Chemistry of Aerosols*, Lewis, Boca Raton.

*Received for review, November 11, 2009*
*Accepted, December 28, 2009*